(Preprint) AAS 22-156

PRECISION POINTING IMPROVEMENTS FOR THE LUNAR RECONNAISSANCE ORBITER CAMERA

Julie Halverson[*], Phil Calhoun[†], Aaron Boyd, Winston Carter, Madeleine Manheim, and Tyler Thompson, [‡]

The Lunar Reconnaissance Orbiter (LRO) was launched in 2009 and, with its seven science instruments, continues to make remarkable discoveries of the Moon. LRO is in a slightly elliptical, polar lunar orbit and nominally maintains a nadir orientation. In early 2018, the Miniature Inertial Measurement Unit (MIMU) was powered off following a fairly rapid decline in the laser intensity on the X axis. An algorithm combining star tracker quaternion differentiated rates and integrated control torque commands in a complementary filter, now provides the onboard rate estimate, replacing the MIMU. One of the science instruments, the LRO Camera (LROC) system, contains a Wide Angle Camera (WAC) and two Narrow Angle Cameras (NAC). The NACs suffer from larger attitude drifts during imaging of the Moon for stereo image processing, resulting from pointing stability degradation of the star tracker derived rates. The controller gains and structural filter were redesigned to attenuate the new disturbances while also maintaining adequate stability and modal suppression. This paper documents the development, testing, and operational implementation of the revised control system parameters, specifically targeted for use during LROC imaging. The new parameters improved pointing performance for LROC.

INTRODUCTION

The Lunar Reconnaissance Orbiter (LRO) was launched on June 18, 2009, with a focus on supporting the extension of human presence in the solar system. The Exploration Mission phase ended in 2010 and LRO became a part of NASA's Science Mission Directorate beginning its Science Mission. LRO is equipped with the following seven instruments: Cosmic Ray Telescope for the Effects of Radiation (CRaTER), Diviner Lunar Radiometer (DLRE), Lyman Alpha Mapping Project (LAMP), Lunar Exploration Neutron Detecter (LEND), Lunar Orbiter Laser Altimeter (LOLA), Lunar Reconnaissance Orbiter Camera (LROC), and the mini-RF technology demonstration. LRO has greatly contributed to our understanding of the Moon and is providing critical data for future human and robotic missions to the moon.

LRO is equipped with ten coarse sun sensors, two star trackers, the miniature inertial measurement unit (MIMU), four reaction wheels, and ten thrusters for momentum management and orbit adjustments. The LRO orbit is an approximately 85 km by 100 km altitude orbit with an inclination of approximately 85 deg and orbital period of 2 hours. During the course of a year the beta angle goes through a full cycle from -90 deg to +90 deg and back to -90 deg, passing through 0 deg twice. At beta angles between -37.5 deg and 37.5 deg, the solar array tracks the sun. Otherwise it remains

[*]Space Sciences Mission Operations, NASA/GSFC, Greenbelt, MD 20771.
[†]Guidance, Navigation, and Control, NASA/GSFC, Greenbelt, MD 20771.
[‡]LROC Science Operations Center at Arizona State University, Tempe, AZ 85281.

parked. Figure 1 is an image of the LRO spacecraft. The attitude control system has four modes of operation: Observing, Momentum Management, Orbit Maintenance, and Sun Safe. The Attitude Control System (ACS) is three-axis stabilized, and the Observing mode provides nadir, off-nadir, and inertial fine pointing in support of science observations, instrument calibrations, and special imaging.[1]

Figure 1: Lunar Reconnaissance Orbiter (Courtesy of NASA/LRO)

LRO CAMERA SYSTEM

The LRO Camera (LROC) system consists of two Narrow Angle Cameras (NACs) that are designed to provide 0.5 meter-scale panchromatic images, and a Wide Angle Camera (WAC) that provides images at a scale of 100 meters/pixel in seven color bands over a 60 km swath at 50 km altitude.[2] Stereo image pairs, provided by the NAC observations of the same point on the ground from different orbits (20 degrees to 40 degrees parallax), are an important measurement in meeting science objectives and also in evaluating future lunar landing sites. Figure 2 is an example of a NAC image, a color shaded relief map of Linné crater produced from LROC stereo pairs.[3] In conjunction with the LOLA instrument, LROC produces digital terrain models (DTM). DTMs are a product that comes from stereo imaging. One stereo pair is four images (two left and two right NAC pairs). One left/right pair is taken at the same time, and combined they make a swath width of approximately 5 km at 50 km altitude. To make a stereo pair, the two left/right image pairs are taken one to four orbits apart of an overlapping area on the Moon to enable the parallax photogrammetry. DTMs are used to analyze terrain and the surface of the moon to provide valuable data for both scientific purposes and future lunar landers. Reference [4] provides an overview of DTM generation and the development of error analysis techniques.

Throughout the mission life there have been sources of jitter that perturbed the NAC stereo images. Early in the mission solar array and high gain antenna motion caused ripples in the NAC stereo images when both were tracking during the observations. Stopping both actuators before and during the images resolved this issue. In 2011 one of the reaction wheels stopped unexpectedly and was powered off, resulting in reduced pointing accuracy. The wheel was eventually powered back on, however there was additional vibration and a high frequency jitter in LROC for particular wheel speed ranges. The vibration and jitter subsided as the wheel ran longer and eventually was not an issue, permitting stereo imaging to continue.

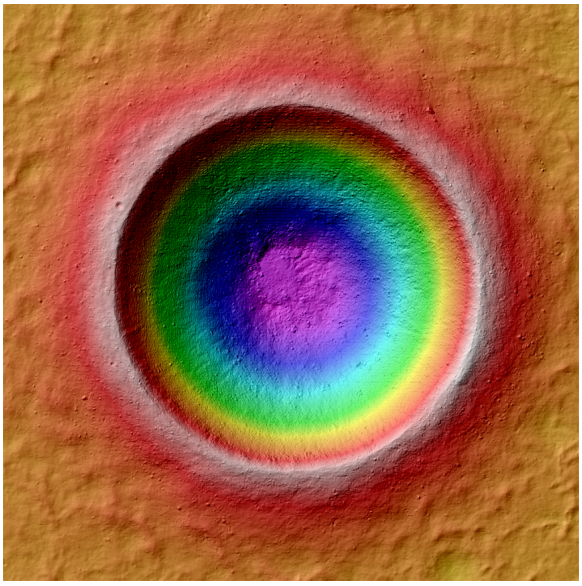

Figure 2: Color Coded Shaded Relief Map of Linné Crater (Courtesy of NASA/GSFC/Arizona State University)

In late 2017, the MIMU laser intensity monitor current on the X axis began declining and it was eventually powered off in March 2018 in hopes to maintain some performance during safing events. A complementary filter, combining star tracker differenced quaternions with integrated control torque commands, was designed to replace the MIMU measurements. With the MIMU powered off, and the complementary filter serving as the rate source, observed amplitudes of spacecraft rotational motion were up to ten times greater than with the MIMU. This affected the LROC NAC Digital Terrain Model pipeline which produces files that are imported by SOCET SET® by BAE systems (see [5]). In the current pipeline, roughly 40% of NAC stereo pairs are not able to be processed into DTMs, 15% are able to be processed with cropped images, and 40% are able to be processed nominally; however, all DTMs created without the MIMU have had an increase in spatial uncertainty in the range of 1 to 4m as compared to uncertainties in the range of 0.5 to 1m with the MIMU.

While registering the latest NAC DTMs to LOLA tracks, some stereo pairs exhibit residuals between LOLA elevation values and the NAC DTMs with root mean square residuals (RMS) greater than 18 m or approximately 25 times larger RMS errors than nominal NAC DTMs acquired when the MIMU was in operation. The mitigation strategies used during DTM processing have included cropping the DTMs to remove difficult-to-control areas, additional parameters in the Multi-Sensor Triangulation algorithm unique to each stereo pair, and creating DTMs at coarser pixel scales to keep the uncertainty to less than 1 pixel. Each mitigation strategy has drawbacks from reduced DTM areal coverage, reduced resolution, or reduced certainty of the DTM.

LROC images, combined with the spacecraft ephemeris information, exhibited angular rotation of 1 to 4 arcsecond total amplitude with periods of 0.14 to 1 seconds with the MIMU. Without the MIMU, the total amplitude of angular rotation has increased to 20 to 40 arcsecond total amplitude with periods of 10 to 15 seconds. The increased spacecraft motion has caused an increase in uncertainty of LROC NAC DTM creation. Figure 3(a) shows the attitude error from the LRO controller

with the MIMU providing the rate estimate and Figure 3(b) shows the attitude error during a stereo image attempt in 2019. The first image of the stereo pair was taken over the last 23 seconds of Figure 3(b). The excursions in the attitude error prevented the resolution of the first image with the second image taken an orbit later. This paper documents the effort to reduce the disturbances dur-

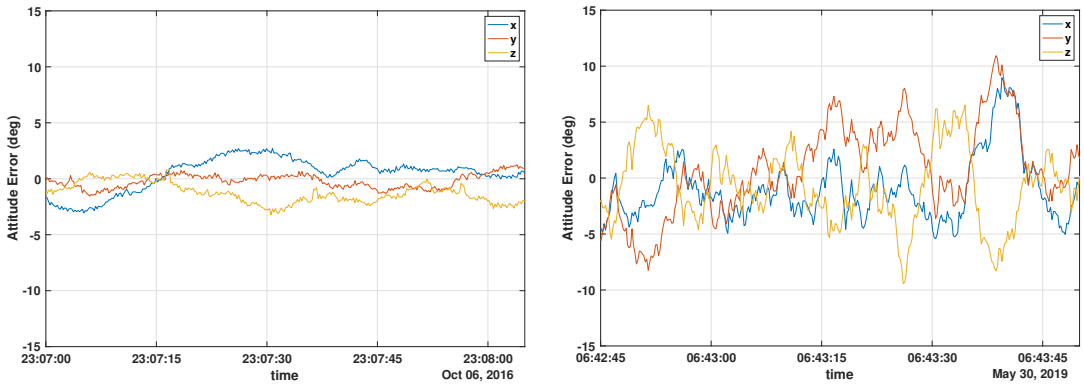

(a) With MIMU (b) Without MIMU

Figure 3: Attitude Error Comparison

ing LROC stereo imaging, such as those described above and those shown in Figure 3(b), through a re-tuning of the LRO onboard attitude controller. The next section includes an overview of the controller along with the design of the new controller parameters. Then testing of the redesigned controller in the LRO high fidelity simulator is provided, followed by inflight results, and finally conclusions and recommendations for future work.

CONTROLLER DESIGN

The LRO controller, given in Equation 1 is a quaternion-feedback, Proportional Integral Derivative (PID) controller with gyroscopic compensation included. $\vec{T_c}$ is the body control torque, I_B is the inertia matrix in the spacecraft body frame, $\vec{\omega}_e$ is the rate error, $\vec{a}_e$ is the attitude error, and k_p, k_I, and k_r are the proportional, integral, and rate gains, respectively. The reaction wheel angular momentum is given as $\vec{h}_W$ and the angular velocity in the body frame is given as $\vec{\omega}_B$. Proportional limiting is applied to the attitude error term, a_e which is the vector part of the error quaternion computed with the estimated quaternion and target attitude quaternion, to constrain the maximum slew rate.

$$\vec{T_c} = I_B(k_r\vec{\omega}_e + k_p \text{proplim}\,[\vec{a}_e] + k_I \int \vec{a}_e) + \vec{\omega}_B \times (I_B\vec{\omega}_B + \vec{h}_W) \tag{1}$$

The nominal PID gains yield a -3db bandwidth of 0.04 Hz, which is more than a decade below the lowest flexible mode frequency. A structural filter, implemented as a third order elliptic filter, is applied to each PID body axis torque, providing modal suppression while maintaining stability.[1]

An extended Kalman filter (EKF) estimates the spacecraft attitude and rate bias using the star tracker quaternions and estimated rates. After the MIMU was powered off, the rate was provided by differentiation of the star tracker quaternions. A star tracker derived rates complementary filter was designed and tested as a replacement for the noisy quaternion only rate estimate. The complementary filter combines star tracker differentiated quaternions and integrated PID filtered and limited control torques, and was uploaded to the spacecraft in December 2018.[6] The star tracker derived

rates complementary filter has performed well onboard, allowing science operations to continue with minimal changes from MIMU-based operations.

After reviewing the attitude errors from several stereo image attempts, disturbances in the frequency range of 0.02 Hz to 0.1 Hz seem to cause the biggest issues in resolving stereo image pairs. Two updates to the controller were proposed to increase the bandwidth first by a factor of 2.5 and then by a factor of 3 to improve attenuation of the disturbances in the identified frequency range, this resulted in an increase in each of the three controller gains which are provided in Table 1 as Redesign A and Redesign B, respectively. The second change was a redesign of the structural filter. The order of the elliptic filter was increased from third to fourth order. The bandwidth was increased along with the steepness of the attenuation at the cutoff frequency in order to accommodate the increase in the controller bandwidth and still maintain stability margins and attenuation of flexible modes. Table 1 lists the nominal and redesigned filter parameters, the redesigned structural filter is used for both sets of new controller gains. Figure 4 shows the frequency response of both the nominal and the redesigned structural filters.

Table 1: Controller Parameters

Parameter	Nominal	Redesign A	Redesign B
k_r (sec^{-1})	0.406	1.015	1.218
k_p (sec^{-2})	0.057	0.356	0.513
k_I (sec^{-3})	0.002	0.014	0.021
Passband ripple (db)	0.1	5	5
Stopband (db)	32	28	28
Frequency bandwidth (Hz)	0.36	0.8757	0.8757

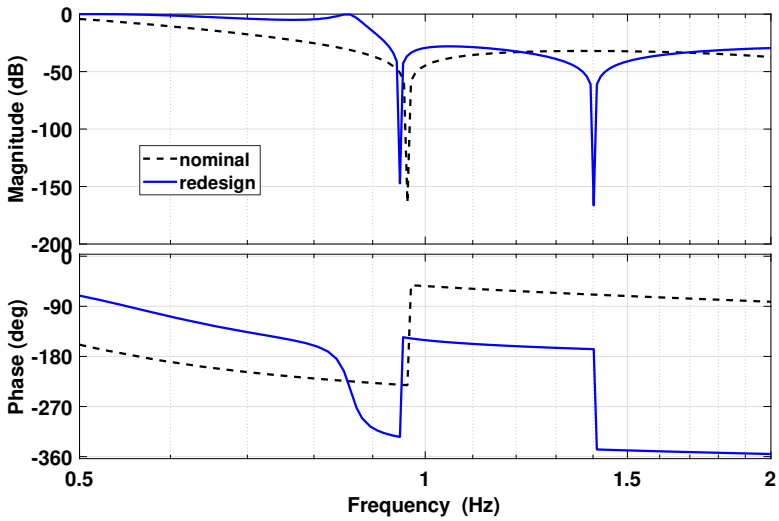

Figure 4: Bode Plot for the Structural Filters

The next step in evaluation of the redesigned controller is a stability analysis. The stability tool, a Matlab based model of the PID control loop, models flexible modes for ten different spacecraft

configurations based on a finite element model. The ten configurations are a combination of five solar array configurations and two fuel fill configurations. In addition, the model determines the minimum stability margins in the presence of inertia variations, flexible mode frequency variations, and flexible mode gain variations (all the variations range over $\pm 20\%$ of the nominal values). Table 2 shows the gain margins, model suppression margins, and phase margins for the nominal and redesigned controllers for nominal flexible body test cases (noted as case 1), the nominal flexible body test cases with the added inertia variations (noted as case 2), and finally the nominal flexible body test cases with the added inertia and flexible mode frequency and gain variations (noted as case 3). As expected, the stability margins decrease from the pre-flight design. During development, the controller design is expected to meet defined stability standards, at least 6 db of rigid body gain margin, at least 12 db of model suppression for all flexible modes, and at least 30 deg of phase margin.[7] Given that LRO is well beyond the prime mission phase and the LROC stereo camera observations take place over a short period of time with no solar array or high gain antenna motion, the reduction in stability margins is an acceptable risk.

Table 2: Stability Margins
1 = Nominal, 2 = Inertia Variation, 3 = Inertia and Flex Variation

	Gain Margin (db)			Modal Sup (db)			Phase Margin (deg)		
Case	X	Y	Z	X	Y	Z	X	Y	Z
Nominal (1)	7.74	7.77	8.27	28.2	31.4	24.4	36.6	36.7	36.7
Redesign A (1)	7.47	7.47	6.80	23.9	25.4	17.3	26.4	26, 6	24.3
Redesign B (1)	3.92	3.91	4.62	20.7	22.2	14.1	22.3	22.6	20.1
Nominal (2)	6.05	6.07	6.65	26.6	29.9	22.8	34.3	34.7	33.1
Redesign A (2)	5.71	5.71	6.31	22.3	23.8	15.7	24.9	25.1	22.8
Redesign B (2)	1.88	1.86	2.85	19.1	20.6	12.5	18.6	19.2	15.7
Nominal (3)	6.03	6.02	6.58	22.2	25.6	21.4	34.2	34.5	32.9
Redesign A (3)	5.67	5.65	6.22	11.7	15.8	5.81	24.8	24.1	22.7
Redesign B (3)	1.84	1.81	2.78	8.69	12.7	2.60	18.4	18.9	15.5

HIGH FIDELITY SIMULATION TESTING

The LRO High Fidelity Simulation (HiFi) is a comprehensive dynamic simulation implemented in Matlab's® Simulink environment. In 2018 the HiFi was upgraded to match the current state of the spacecraft, the inertia and mass were updated to reflect fuel usage over the life of the mission from momentum unloading and orbit maintenance. The reaction wheel and star tracker truth model noise parameters were updated to match flight performance. The HiFi was enhanced to incorporate real data for initialization and to read spacecraft ephemerides. The complementary filter algorithm, which provides the rate estimate with the MIMU powered off, was incorporated into the HiFi and tested prior to uploading the algorithm to the spacecraft in late 2018.[6]

The HiFi was used to test and evaluate the redesigned controller parameters. First, a disturbance was created that could be included during the time when LRO was on target. The disturbance was modeled as band-limited white noise using a fourth order bandpass filter over the frequency range of

0.02 to 0.1 Hz. White noise was input to the disturbance model and the variance was tuned until the desired disturbance was achieved. A rate limiter was included so that the disturbance would ramp up over a minute and similarly ramp down over a minute. Figure 5 is an example of the disturbance profile. The disturbance was added to the other external disturbance torques modeled in the HiFi truth model.

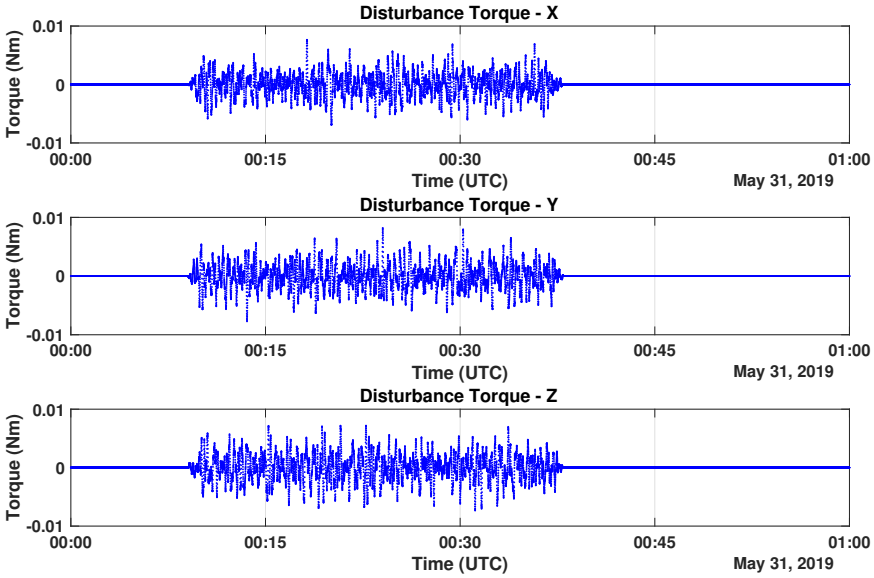

Figure 5: HiFi Added Disturbance Torque

The LRO controller parameters are accessed in the flight software through tables. The structural filter is implemented in the flight code, and in the HiFi, as cascaded second order filters. The elliptic filter with the design parameters provided in Table 1 is split into two second order filters, assigning two poles and zeros to each filter, and then converting into discrete filters of the format provided in equation 2, where the index i represents each of the three spacecraft axes. The numerator and denominator coefficients are provided in Table 3. Note that the coefficients are the same for all three axes.

$$\frac{\text{Output}}{\text{Input}} = \frac{\mathrm{B}_{i,1} + \mathrm{B}_{i,2}\mathrm{z}^{-1} + \mathrm{B}_{i,3}\mathrm{z}^{-2}}{1 + \mathrm{A}_{i,1}\mathrm{z}^{-1} + \mathrm{A}_{i,2}\mathrm{z}^{-2}} \tag{2}$$

The redesigned gains from Table 1 are also inserted into a flight software table along with the

Table 3: Flight Software Filter Coefficients

Parameter	Filter 1	Filter 2
$\mathrm{B}_{i,1}$	0.2766	0.2766
$\mathrm{B}_{i,2}$	−0.2033	0.1050
$\mathrm{B}_{i,3}$	0.2766	0.2766
$\mathrm{A}_{i,1}$	−0.9198	−1.2825
$\mathrm{A}_{i,2}$	0.9573	0.6771

controller integral error limit. The integral error limit is reduced in proportion to the increase in

the proportional gain, however the factor was increased by an additional 50% for both redesigned control parameters to ensure the integrator would not saturate.

The typical slew profile for an LROC stereo observation is to slew to the target, wait two minutes to allow settling, take the image over an approximately 30 second window, and then slew back to nadir. For the purposes of the simulation, the time on target was extended in order to better evaluate the performance of the redesigned controller. The slew scenario was set up to first slew to the actual target five minutes into the simulation using the nominal controller parameters. The disturbance torque was ramped in after arriving on target. The nominal controller parameters are in place for the first 14 minutes on target, then the controller swaps to the redesigned parameters for the next 14 minutes, the disturbance is ramped down, the controller swaps back to the nominal parameters and holds for two minutes and then the spacecraft slews back to nadir 39 minutes into the simulation. Figures 6 and 7 show the attitude error in the X axis for Redesign A and Redesign B (the other axes are similar). The plot on the left in each figure shows an expanded view and the plot on the

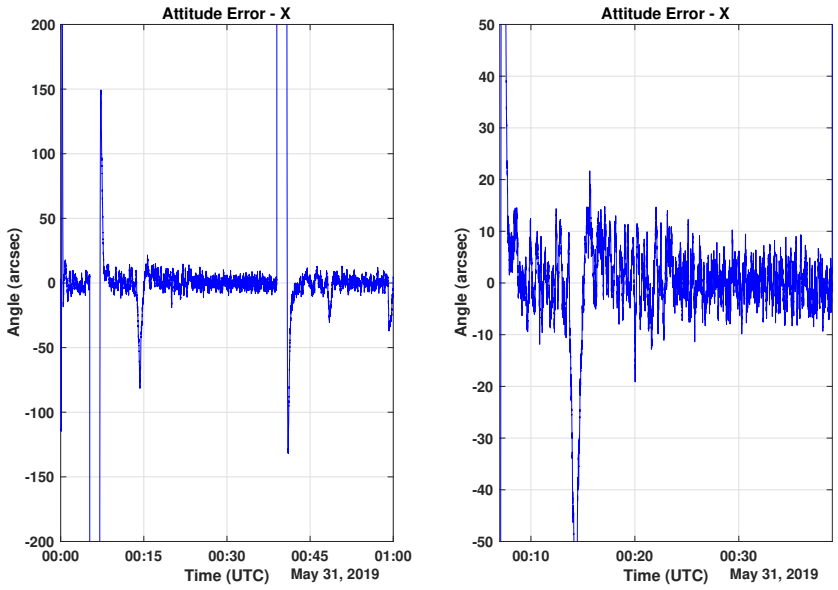

Figure 6: Simulated Attitude Error in the X Axis - Redesign A

right has a reduced scale. The transient response at fifteen minutes into the simulation is due to a reaction wheel crossing through zero. The improvement resulting from the redesign is apparent but is clearer in Redesign B. Figure 8 shows seven minutes of the X axis attitude error with the nominal parameters and seven minutes with the redesigned parameters overlaid, again Redesign B shows the most improvement. The root mean square error for the nominal span in Figure 8 is 6.36 arcseconds, it is 3.58 arcseconds for Redesign A, and 3.02 for Redesign B .

The inflight timeline was adjusted to increase the on target time for LROC stereo imaging, in order to give the controller time to settle and observe improvements in performance. Following the slew to the target, there would be a four to five minute wait time to settle at the target with the nominal controller parameters, then the redesigned controller parameters would be activated followed by another four to five minute wait to let the controller settle, then a one minute window is inserted during which LROC takes the image. The nominal controller parameters are reactivated after the image followed by a two minute wait to allow settling before slewing back to nadir. The

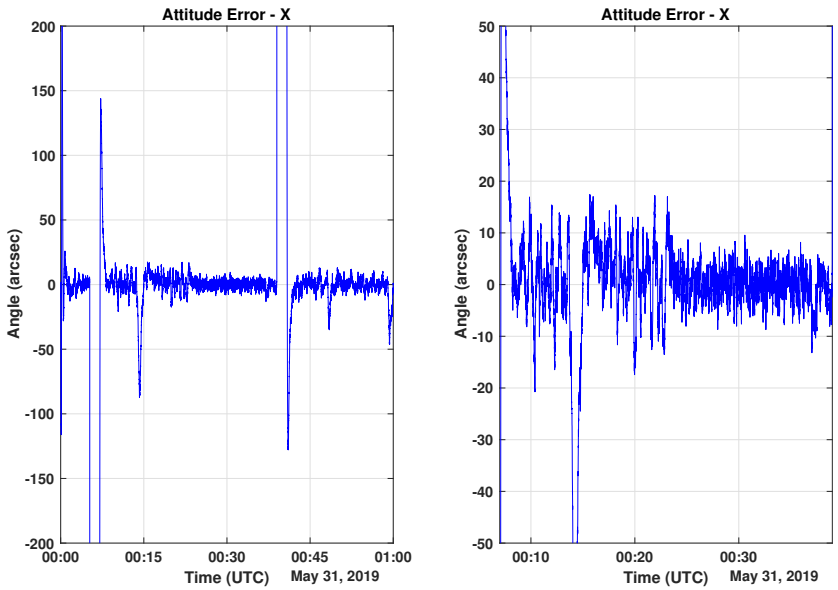

Figure 7: Simulated Attitude Error in the X Axis- Redesign B

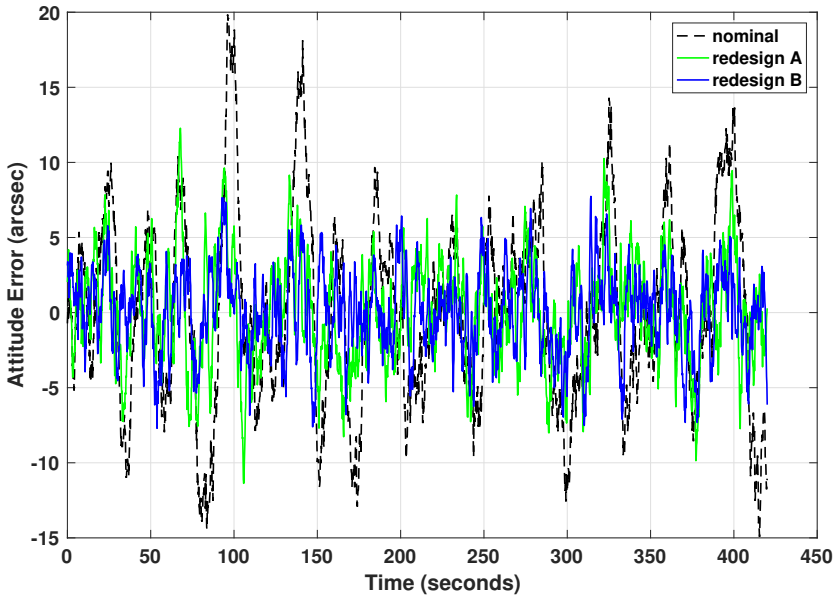

Figure 8: Simulated X Axis Attitude Errors Overlaid

LROC timeline was tested in the HiFi with similar results as those given in 6 and 7. The LRO flight software team also tested the slew scenario in the flight software simulator and confirmed that the redesigned controller parameters loaded as expected and all commands executed as planned.

INFLIGHT TESTING

For each of the inflight tests, the LROC team chose a target, and a slew was designed for that target. The slew was first evaluated on the ground to confirm that neither star tracker would be occulted and that no thermal or power violations would occur on the spacecraft. The solar array

and high gain antenna are stopped three minutes prior to the slew start and remain stopped until two minutes after returning to nadir pointing. The slew plan then followed the timeline given above. Figure 9(a) shows the actual attitude control error in the X axis when using the Redesign A controller parameters. The slew completes at about 05:19, the new parameters are activated just before 05:22, and the image is taken just before 05:26. The nominal controller parameters are reactivated just before 05:27 followed by the slew back after the two minute wait. Figure 9(b) shows the inflight test results using the Redesign B controller parameters. The slew completes at about 12:47 and the redesigned controller parameters are activated at approximately 12:51. There is a reaction wheel zero crossing just past 12:52. The controller settles after the zero crossing and the image is taken at approximately 12:56. The nominal controller parameters are activated at approximately 12:57 followed by the slew back to nadir after the two minute wait to allow the controller parameters to settle. The excursions during these events, with the nominal controller parameters, were not

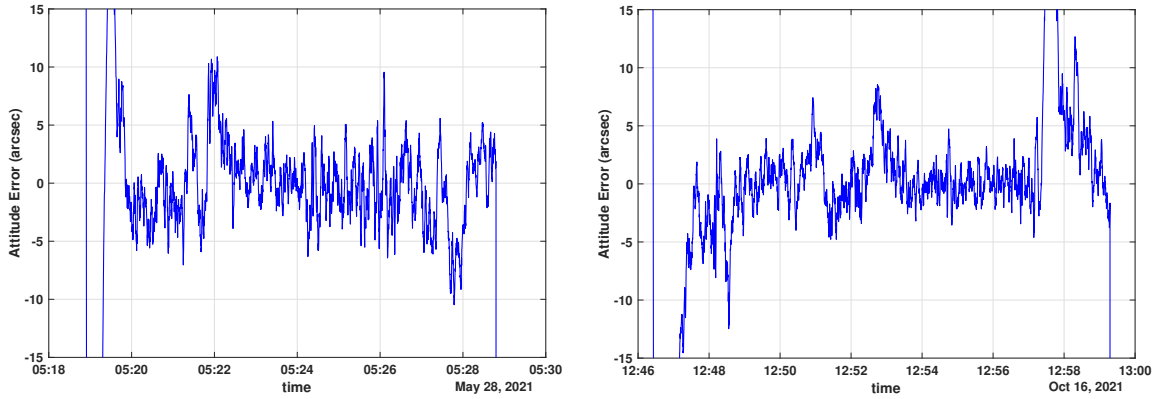

(a) Redesign A

(b) Redesign B

Figure 9: Inflight Testing of Redesigned Controller Parameters

as pronounced as those in Figure 3(b). The activation of the Redesign A parameters shows little improvement. The Redesign B does show improvement, with the attitude error below 3 arcseconds during the interval with the image.

During all inflight test slews, the spacecraft was monitored in real time to ensure that no unexpected behavior occurred with the new parameters, such as saturating the reaction wheel torque. Figure 10 shows the reaction wheel torques for all four reaction wheels for the Redesign B parameters, all of which are well within the 0.2 Nm torque limit. The torques from Redesign A were slightly less, but with a similar profile. Figure 11 shows the integral error for the Redesign B parameters, the time period with the redesigned controller parameters active remains well within the revised saturation limit of 0.27 deg-sec. The results were similar with the Redesign A parameters.

The LROC images observed with the Redesign A parameters show little to no improvement in the 0.02 to 0.1 Hz frequency range, but the motion appears somewhat more regular, while the Redesign B parameters has resulted in a 10%-20% reduction of spacecraft motion amplitude during NAC imaging when compared to using the nominal controller parameters. The Redesign A parameters resulted in only a modest reduction in stability as shown in Table 2, whereas the Redesign B parameters are more aggressive. The aggressive approach provided more improvement in NAC imaging since powering off the MIMU. Figure 12 is one example of a single NAC image (left NAC) of the west wall of the Lavoisier crater with the Redesign B parameters.

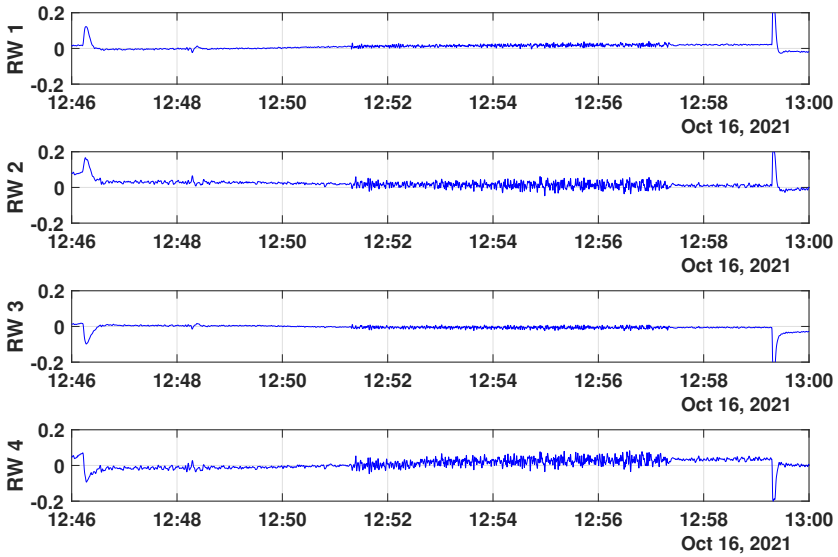

Figure 10: Reaction Wheel Torques (Nm) During Inflight Test

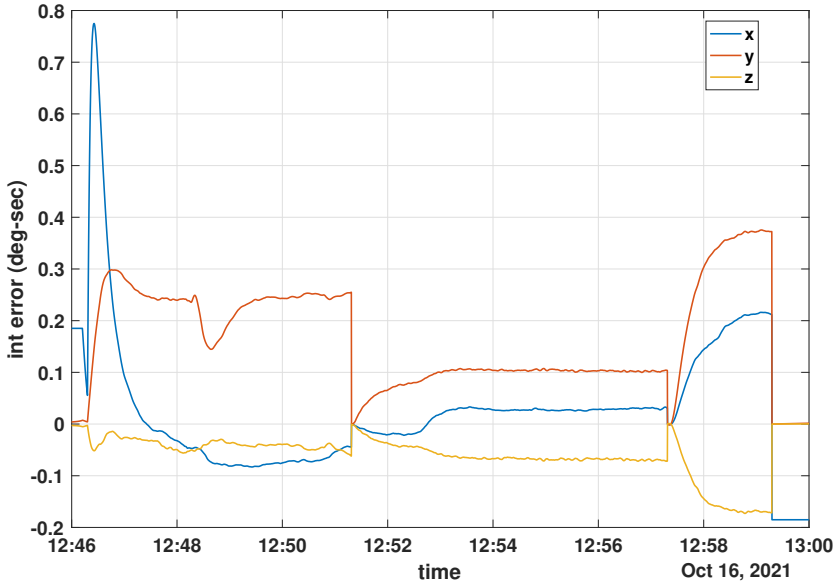

Figure 11: Integral Error During Inflight Test

CONCLUSIONS AND FUTURE WORK

The LRO attitude control system parameters were tuned in an attempt to attenuate disturbances observed by LROC after the MIMU was powered off. Two sets of parameters were proposed and tested, the first of which resulted in a modest decrease in pre-launch stability margins while the second set was more aggressive. The redesigned controllers were tested on the ground in a high fidelity simulator. A disturbance was added to the simulator truth model to mimic the motion observed by LROC. Both redesigned controllers resulted in improvements in the attitude control error in the simulator. Next the new parameters were formulated into flight software tables and loaded to the spacecraft. Inflight tests were conducted, first with the modest parameter change followed by the

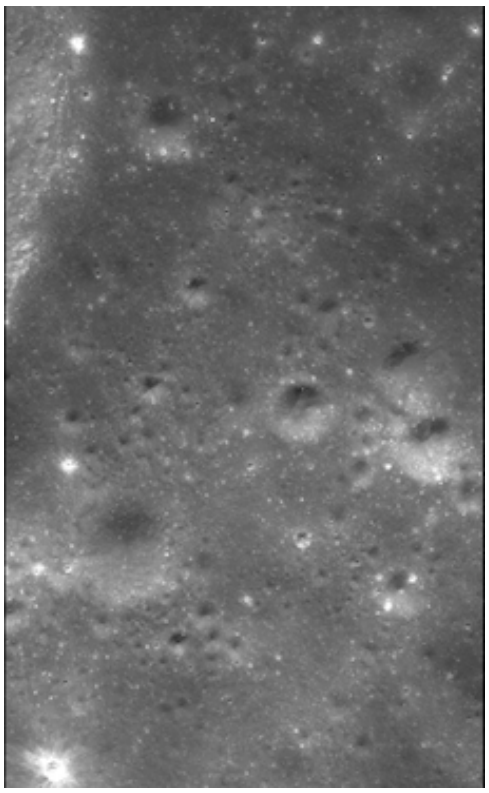

Figure 12: NAC Left Partial Image of the West Wall of the Lavoisier Crater Using Redesign B Parameters. (Courtesy of NASA/GSFC/Arizona State University)

more aggressive parameter change. The modest parameter set resulted in little to no improvement in flight, while the more aggressive parameters did show a reduction of spacecraft amplitude motion. Additional tests will be conducted onboard with the second set of parameters, with the expectation of increasing the number of NAC stereo pairs that can be processed into DTMs. A third and final set of control parameters is also being considered, that is slightly more aggressive than the second set. Given that the reaction wheels were well within torque limits, there is sufficient control authority to increase the gains a bit further, resulting in even more improvement in the production of NAC stereo images.

REFERENCES

[1] P. Calhoun and J. Garrick, "Observing Mode Attitude Controller for the Lunar Reconnaissance Orbiter," *20th International Symposium on Space Flight Dynamics*, Annapolis, Maryland, September 2007.

[2] M. S. Robinson, S. M. Brylow, M. Tschimmel, D. Humm, S. J. Lawrence, P. C. Thomas, B. W. Denevi, E. Bowman-Cisneros, J. Zerr, M. A. Ravine, M. A. Caplinger, F. T. Ghaemi, J. A. Schaffner, M. C. Malin, P. Mahanti, A. Bartels, J. Anderson, T. N. Tran, E. M. Eliason, A. S. McEwen, E. Turtle, B. L. Jolliff, and H. Hiesinger, "Lunar Reconnaissance Orbiter Camera (LROC) Instrument Overview," *Space Sci Rev*, Vol. 150, March 2010, pp. 81–124.

[3] "Lunar Reconnaissance Orbiter Camera (LROC)," website. http://lroc.sese.asu.edu/.

[4] T. Trana, M. R. Rosiek, R. A. Beyer, S. Mattson, E. Howington-Kraus, M. Robinson, B. A. Archinal, K. Edmundson, D. Harbour, E. Anderson, and t. LROC Science Team, "Generating Digital Terrain Models Using LROC NAC Images," *ASPRS/CaGIS 2010 Fall Specialty Conference*, Orlando, Florida, November 2010.

[5] "SOCSET SET®," website. https://www.geospatialexploitationproducts.com.

[6] J. Halverson, P. Calhoun, O. Hsu, J.-E. Dongmo, R. Besser, B. Ellis, R. DeHart, Y. Tedla, S. Rosney, and S. Snell, "Testing of the Lunar Reconnaissance Orbiter Attitude Control System Re-Design Without a Gyro," *AAS Guidance and Control Conference*, No. AAS 19-108, Breckenridge, Colorado, February 2019.

[7] "Rules for the Design, Development, Verification, and Operation of Flight Systems," website. https://standards.nasa.gov.